Translational Stroke Research
https://doi.org/10.1007/s12975-025-01343-3

RESEARCH

Photobiomodulation Promotes Early Recovery of Olfactory Function and Modulates Neuroprotective Gene Expression in a Mouse Model of Ischemic Stroke

Reham A. Shalaby[1] · Acquah Emmanuel[1] · Fatemeh Dehgan Nezhad[1] · Kohinur Akter[5] · S. M. Abdus Salam[3] · Jawoon Yi[2] · Sang Seong Kim[1] · Jihwan Park[2] · Hyuk Sang Kwon[1,5,6] · Kyung Hwa Lee[3] · Young Ro Kim[4,7] · Euiheon Chung[1,5,6]

Received: 22 October 2024 / Revised: 25 December 2024 / Accepted: 4 March 2025

Abstract

Ischemic stroke often leads to neurological deficits, including olfactory dysfunction, which can significantly diminish quality of life. Photobiomodulation (PBM) has emerged as a promising therapeutic strategy for enhancing post-stroke recovery, although the molecular mechanisms, particularly regarding gene expression change, are not yet fully understood. This study investigates the long-term effects of photothrombosis (PT) on olfactory function and the olfactory bulb (OB) microenvironment, with a focus on PBM's efficacy during both early and late phases. In a mouse OB PT stroke model, PBM therapy (808-nm laser, 40 J/cm^2 fluence, 325 mW/cm^2, 2 min daily) was applied from day 2 to day 7 post-PT. Olfactory function was monitored from pre-stroke through day 28 using the buried food test (BFT), and MRI scans were performed on days 7 and 28 to assess tissue damage. RNA sequencing (RNA-seq) and reverse transcription quantitative PCR (RT-qPCR) were conducted on day 7 to evaluate gene expression changes, with additional RT-qPCR analyses performed on day 28. PBM significantly accelerated olfactory function recovery by day 14, with full recovery maintained through day 28. Despite functional recovery, MRI results indicated persistent infarction at 28 days. RNA-seq identified upregulation of neuroprotective genes, including *Gpr39* and *Or4m1*, following PBM treatment, suggesting enhanced gene expression related to acute-phase recovery. However, the impact of PBM on gene expression and functional recovery appeared to wane in the later stages of recovery. These findings underscore PBM's potential to enhance early-stage recovery in ischemic stroke, though its benefits may be more limited in the chronic phase.

Introduction

Ischemic stroke often leads to a range of neurological impairments, including olfactory dysfunction, for which effective treatment options remain limited. The olfactory bulb (OB) plays a critical role in processing olfactory information, and its complex architecture and diverse cell types make it particularly susceptible to ischemic damage [1]. Photobiomodulation (PBM), a non-invasive therapy using low-level light, has emerged as a promising approach to

✉ Young Ro Kim
yrkim@mgh.harvard.edu

✉ Euiheon Chung
ogong50@gist.ac.kr

[1] Department of Biomedical Science and Engineering, Gwangju Institute of Science and Technology, Gwangju, South Korea

[2] School of Life Sciences, Gwangju Institute of Science and Technology, Gwangju, South Korea

[3] Department of Pathology, Hwasun Hospital and Medical School, Biomedical Sciences Graduate Program (BMSGP), Chonnam National University, Gwangju, South Korea

[4] Department of Radiology, Harvard Medical School, Boston, MA, USA

[5] AI Graduate School, Gwangju Institute of Science and Technology, Gwangju, South Korea

[6] Present Address: Department of Physics and Photon Science, Gwangju Institute of Science and Technology, Gwangju, South Korea

[7] Athinoula A. Martinos Center for Biomedical Imaging, Massachusetts General Hospital, Boston, USA

Published online: 13 May 2025

improve neurological function after stroke by modulating inflammatory responses and enhancing glial and vascular factors [2]. However, the molecular mechanisms by which PBM exerts its therapeutic efficacy, particularly in specific brain regions like the OB, remain poorly understood.

Advances in high-throughput sequencing technologies have shed light on the molecular processes involved in stroke pathology, including neuronal necrosis, ischemic injury, and inflammation [3, 4]. These technologies enable the exploration of gene expression changes that occur after stroke, potentially revealing therapeutic targets to mitigate neurological deficits.

Previous studies have demonstrated the efficacy of PBM in ischemic stroke by improving the post-stroke microenvironment and inhibiting ischemia-induced vascular endothelial senescence [5, 6]. In models of neurodegenerative diseases such as Alzheimer's disease (AD), PBM has been shown to reduce neuroinflammation, oxidative stress, and amyloid-β plaque deposition, leading to improved cognitive function [7, 8]. PBM has also been effective in treating traumatic brain injury (TBI), resulting in increased cerebral volume and perfusion, as well as enhanced functional connectivity and cognitive abilities [9, 10].

Animal models are essential for understanding disease mechanisms and testing therapeutic interventions in stroke research. While the middle cerebral artery occlusion (MCAO) model is commonly used to replicate ischemic stroke [11], the photothrombotic (PT) stroke model offers advantages for inducing targeted, permanent ischemia in specific brain regions, such as the OB. The PT model allows for precise control over infarct size and location, facilitating investigations of molecular signatures unique to different brain regions following stroke [12, 13].

Recent research has highlighted the role of specific genes, such as *Gpr39* and olfactory receptor family 4 subfamily M member 1 (*Or4m1*), in the brain's response to ischemic injury. *Gpr39*, expressed in pericytes surrounding capillaries, regulates microvascular perfusion, and its knockout in mice leads to worsened stroke outcomes, including larger infarcts and reduced neurological recovery [14]. Similarly, the downregulation of *Or4m1* in the brain after TBI may contribute to neurological complications [15], emphasizing a more significant role of olfactory receptors in brain pathology than previously understood.

In this study, we used the PT stroke model to induce ischemic damage in the OB and administered daily PBM therapy to evaluate its therapeutic effects on functional recovery and molecular changes within the OB. Behavioral assessments, immunohistochemistry (IHC), MRI imaging, and RNA sequencing (RNA-seq) were employed to assess the impact of PBM during both the early and late stages of ischemic stroke recovery. To our knowledge, this is the first study to evaluate olfactory function at later time points following PT stroke and to apply RNA-seq to examine PBM's effects in an OB stroke model. We aim to elucidate the mechanisms by which PBM restores olfactory function, potentially uncovering novel therapeutic strategies for treating post-stroke olfactory dysfunction and other neurodegenerative diseases.

Methods

All experimental protocols followed the guidelines of the Institutional Animal Care and Use Committee (IACUC) at Gwangju Institute of Science and Technology (GIST), Korea. The experimental protocols were approved by the GIST IACUC under protocol # GIST-2024–046. We used 75 C57BL/6 male mice aged between 10 and 14 weeks.

Buried Food Test for Olfactory Function Measurement

The buried food test (BFT) was performed according to the previously published protocol [16] and our previously published study [2]. Adaptation to food was achieved by introducing the food pellets with fresh odor daily to the mice for 1 week. On the test day, animals were fasted (except for water) for 18 h and then introduced to a clean mouse cage where an odorous food pellet (RodFeed, DBL, Chungcheongbuk-do, South Korea) was randomly embedded under the 3 cm thickness of clean bedding. Then, latency in the food search time was measured, which was repeated three times for each BFT session. The first BFT after PT was performed 3 days after the PT since certain mice were inactive after their PT surgeries, so the time was taken to allow the mice to recover. We measured the body weight before each BFT to assess the weight fluctuation after 18 h of fasting. The BFT was conducted on day 1 before the PT induction to obtain the baseline which was followed by the BFTs on days 3, 7, 14, 21, and 28 post-PT. Ten mice were used to assess the olfactory function from early- to late-stage post-PT.

Olfactory Bulb Photothrombosis

Photothrombosis (PT) was performed on day 0 for the PT and PT + PBM groups. After anesthetizing the mice, an incision was made in the scalp over the olfactory bulb (OB) area between the eyes, and the periosteum was removed. A 4-mm coverslip was placed over the OB area and secured with adhesive. Mice received a retro-orbital injection of 20 mg/kg rose Bengal dye, followed by illumination with a 532-nm green laser over the OB for 15 min in a dark room. Control mice underwent the same procedure without the rose Bengal

injection. Body temperature was maintained at 37 ± 0.5 °C throughout the procedure.

Photobiomodulation Treatment

Photobiomodulation (PBM) therapy was administered daily from day 2 to day 7 post-PT using an 808-nm laser with a fluence of 40 J/cm^2 (325 mW/cm^2 for 2 min per session). The laser beam diameter was 4.17 ± 0.07 mm. PBM was performed in a dark room, with body temperature maintained at 37 ± 0.5 °C. A protective mask with an opening over the OB area was used to shield the surrounding tissues from unnecessary light exposure.

Brain Tissue Sampling and Histology

On days 7 and 28 post-PT, mice were euthanized, and brains were harvested after perfusion with 4% paraformaldehyde (PFA). Brains were fixed in 10% neutral-buffered formalin for 3 days and then embedded in paraffin for histological examination and MRI imaging. For RNA-seq and RT-qPCR analyses, OB tissues were preserved in RNAlater solution at − 80 °C until processing.

Immunohistochemistry (IHC)

Paraffin-embedded brain Sects. (3 µm thick) were subjected to IHC staining. Sections were stained using antibodies against glial fibrillary acidic protein (GFAP; 1:400 dilution, Dako), ionized calcium-binding adaptor molecule 1 (IBA-1; 1:400 dilution, Synaptic Systems), and CD31 (1:200 dilution, Dako) using the Bond-max system (Leica Microsystems). Negative controls were processed without primary antibodies. Stained slides were evaluated by a pathologist (KHL) and were digitized using a slide scanner (Aperio ScanScope CS System, Leica Microsystems). For the analysis of IHC, three non-overlapping ROIs in the stained images were randomly selected to capture the heterogeneous distribution of each olfactory bulb. These ROIs were constrained to lie within ~200 µm of the ischemic lesion, corresponding to the peri-infarct area surrounding the lesion followed by analysis using ImageJ (Fiji) software for quantitative evaluation. Twenty-four mice were utilized for the IHC for day 7 and day 28 in PT and PT + PBM groups.

MRI Imaging

T2-weighted images of mouse olfactory bulbs were acquired at 7 and 28 days post-PT for both PT and PT + PBM groups using a Bruker Biospec 9.4 T Console Avance Neo MRI system with a 210 mm bore size. Fixed brain samples were carefully positioned within the MRI bore to ensure optimal imaging of the olfactory bulb. A specialized surface RF coil, designed specifically for mouse brain imaging, was employed to capture high-resolution images of the olfactory bulb's fine structure. 3D fast spin-echo acquisition was performed using the following parameters: TR = 500 ms, TE = 32 ms, and a RARE factor of 16. The field of view was set to 30 × 30 × 30 mm^3 with an isotropic resolution of 0.1 mm. Twenty mice were used in MRI for OB volume measurement at day 7 and day 28 for PT and PT + PBM groups.

RNA Isolation and Sequencing

Total RNA was extracted from OB tissues on day 7 post-PT using TRIzol reagent (Invitrogen), followed by DNase treatment (Promega) and purification. RNA quality was assessed using an Agilent Bioanalyzer. RNA-seq libraries were constructed using the TruSeq Stranded Total RNA Gold Library Kit (Illumina) and sequenced on an Illumina NovaSeq 500 platform to generate 150-nucleotide paired-end reads. Nine mice were utilized for RNA sequencing, with three allocated to each group: control, PT, and PT + PBM.

Reverse Transcription Quantitative PCR (RT-qPCR)

Total RNA extracted from OB tissues on days 7 and 28 post-PT was reverse transcribed into cDNA using the High-Capacity cDNA Reverse Transcription Kit (Thermo Fisher Scientific). RT-qPCR was performed using gene-specific primers for Gpr39 and Or4m1 (Table 1), with GAPDH as the internal control. Reactions were carried out in triplicate using amfiSure qGreen Q-PCR Master Mix (GenDepot) on a Bio-Rad CFX96 real-time PCR system. Relative gene expression levels were calculated using the $2^{-\Delta\Delta Ct}$ method. We used 12 mice in RT-qPCR for PT and PT + PBM for day 7 and day 28.

Table 1 RT-qPCR primer sequences

Gene	Forward 5′ to 3′	Reverse 5′ to 3′
OR4M1	ACCACACCCAGCTATGCTCT	TGAAGGGATGACAAATGGCAAT
GPR39	CCATCCATCTACATTTATGC	ACTTCCTTGTTTCTCAATGT

Statistical Analysis

Data are presented as mean ± standard deviation (SD). Statistical analyses were performed using one-way analysis of variance (ANOVA) and two-way ANOVA with GraphPad Prism software. Comparisons were tested for normality and homogeneity of variances. A *P*-value of less than 0.05 was considered statistically significant.

Results

The Influence of PBM on the Microenvironment from Early- to Late-Stage Post-PT

Figure 1 presents the IHC analysis of glial fibrillary acidic protein (GFAP), a marker for astrocytes, and ionized calcium-binding adaptor molecule 1 (IBA-1), a marker for microglia/macrophages, to assess cellular activation in the

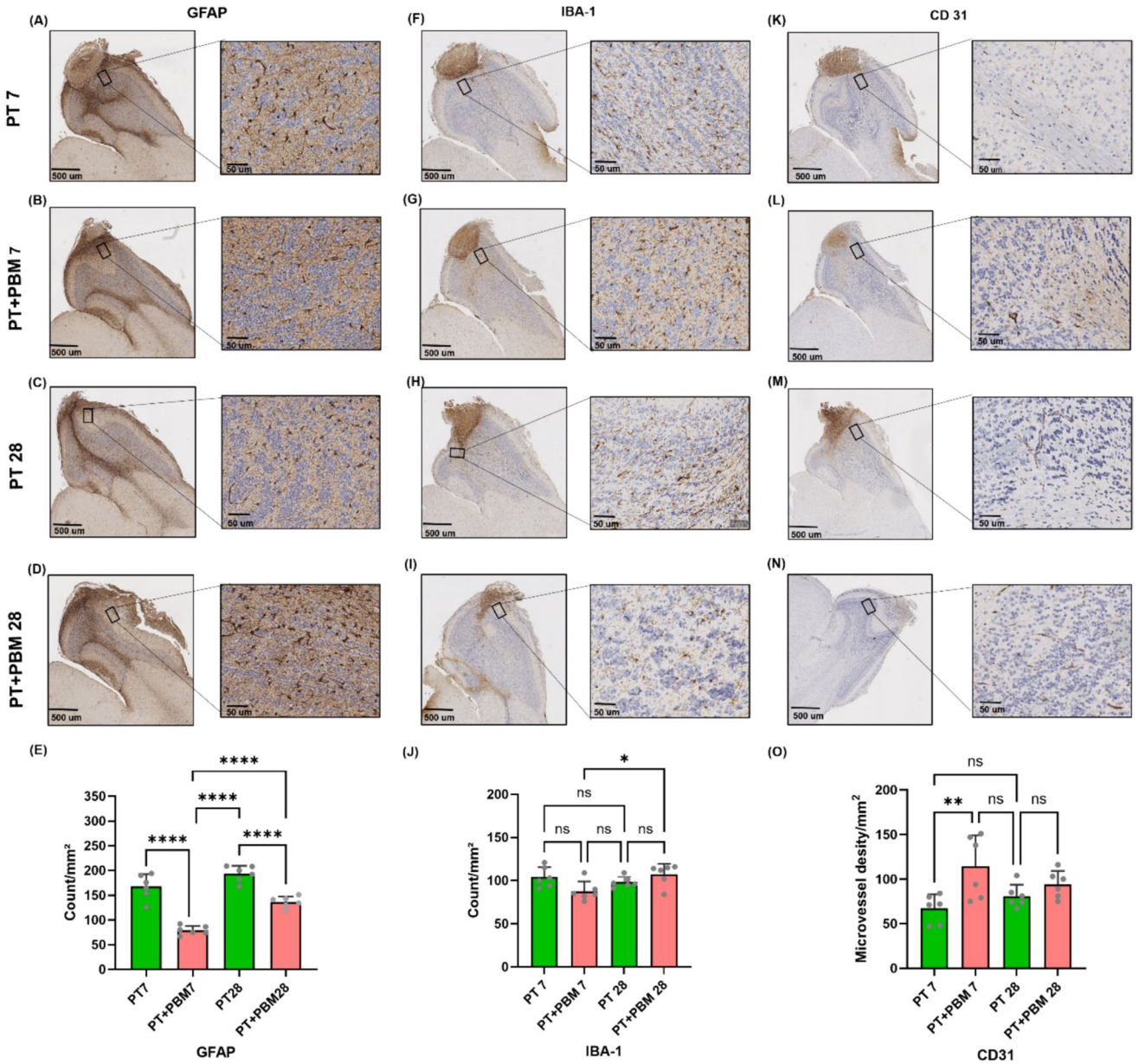

Fig. 1 Impact of PBM on astrocyte and microglial activation and microvessel density in the olfactory bulb following PT at day 7 and day 28. **A**–**D** GFAP staining with high magnification. **F**–**I** IBA-1 staining with high magnification; **K**–**N** CD31 staining with high magnification. **E**, **J**, and **O** Quantitative analysis of GFAP, IBA-1 positive cells, and microvessel density. $*P<0.05$, $***P<0.001$, $****P<0.0001$; ns-not significant). Scale bars, 500 µm and 50 µm. $n=6$ per group

olfactory bulb following photothrombosis (PT) and subsequent photobiomodulation (PBM) treatment at early and late stages post-ischemic stroke.

GFAP staining (Fig. 1A–D) reveals a pronounced increase in astrocytic activation in both the PT 7 (A) and PT 28 (C) groups, consistent with the typical astroglial response to ischemic injury. In contrast, the PT + PBM 7 (B) and PT + PBM 28 (D) groups exhibit a marked reduction in GFAP expression compared to their untreated counterparts, indicating that PBM effectively attenuates astrocyte activation. The quantitative analysis of GFAP-positive cells (Fig. 1E) demonstrates a statistically significant reduction in astrocyte activation in the PBM-treated groups at both 7 and 28 days post-injury, suggesting that PBM mitigates astrocytic reactivity, potentially contributing to its neuroprotective effects in the ischemic olfactory bulb.

IBA-1 staining (Fig. 1F–I) indicates minimal changes in microglial activation between the PT and PBM-treated groups at both time points. The quantitative analysis (Fig. 1J) shows no statistically significant differences between groups at either the early or late stages post-injury, with the exception of a modest reduction at day 7 of PT + PBM compared with day 28 of PT + PBM. These results suggest that PBM has a limited impact on microglial activation during the recovery process.

As shown in Figure for CD31 staining, a marker of endothelial cells, PBM revealed differences in microvessel density at early and late-stage post-ischemic stroke. At 7 days post-PT, there was a significant increase in the microvessel density in the PBM-treated group compared to the untreated PT group, indicating enhanced angiogenesis due to PBM therapy, while there was no significant difference observed at day 28 between PT and PT + PBM group, indicating that PBM's effect on the vascular density may diminish over time.

Overall, these findings indicate that PBM treatment significantly reduces astrocyte activation following ischemic stroke, highlighting its potential neuroprotective role. However, PBM appears to have a less pronounced effect on microglial activation, suggesting that its primary mechanism of action may involve modulating astrocytic responses rather than microglial activity during recovery from ischemic injury. Additionally, PBM is more effective at promoting microvessel density in the early stages after ischemic stroke, with a reduced impact in the later stages.

PBM Accelerates the Recovery in the Early-Stage Post-PT

Figure 2 illustrates the effects of PBM on olfactory function, as assessed by the buried food test, over 28 days following PT. The latency to find the food pellet was measured as an indicator of olfactory function impairment and recovery.

In the PT group (Fig. 2B), there was a significant increase in the latency time to locate the food pellet on day 3 (D3) compared to baseline (D-1), indicating olfactory dysfunction induced by the PT stroke. This impairment persisted at days 7 (D7), 14 (D14), 21 (D21), and 28 (D28), although no statistically significant differences were observed between these later time points and baseline (ns), suggesting partial recovery of function over time.

In contrast, the PBM-treated group (Fig. 2B) demonstrated a faster recovery of olfactory function. While there was a significant increase in latency at D3 and D7 compared to baseline, the olfactory function was restored to near-baseline levels by D14, with no significant differences observed at D14, D21, or D28 (ns). These findings suggest that PBM accelerates the recovery of olfactory function in the early stages post-PT, effectively mitigating the stroke-induced impairment by D14.

Overall, the data indicate that PBM treatment has a therapeutic effect on olfactory function recovery following PT-induced stroke, particularly in the acute phase, suggesting that PBM may preserve or restore sensory function in the context of ischemic brain injury.

PBM Reduces Olfactory Bulb Damage and Preserves Volume Following PT

The MRI data presented in Fig. 3 demonstrate the effect of PBM on reducing ischemic damage in the olfactory bulb OB following PT. In Fig. 3A, the damaged volume (in mm^3) at 7 and 28 days post-PT is presented for the PT and PT+PBM groups. The PBM-treated groups exhibit a reduction in damaged volume at both time points compared to the PT-only groups, although the difference is not statistically significant. Figure 3B presents the damaged volume as a percentage of total OB volume; the PBM treatment leads to a significant reduction in the damaged volume fraction at day 7 post-PT compared to the untreated PT group, while no significant difference was observed between both groups at day 28. Figure 3C illustrates the whole OB volume in cubic millimeters. PBM treatment significantly preserves the overall OB volume at 7 days post-PT compared to the PT group, indicating a neuroprotective effect in the early phase of recovery. However, by 28 days post-PT, there is no statistically significant difference in OB volume between the groups. Figure 3D shows a representative MRI image of the OB, with arrows indicating the damaged region.

Collectively, these findings suggest that PBM treatment effectively reduces the extent of ischemic damage and preserves OB volume during the acute phase of recovery post-PT, with diminished effects observed in the later stages of recovery (28 days).

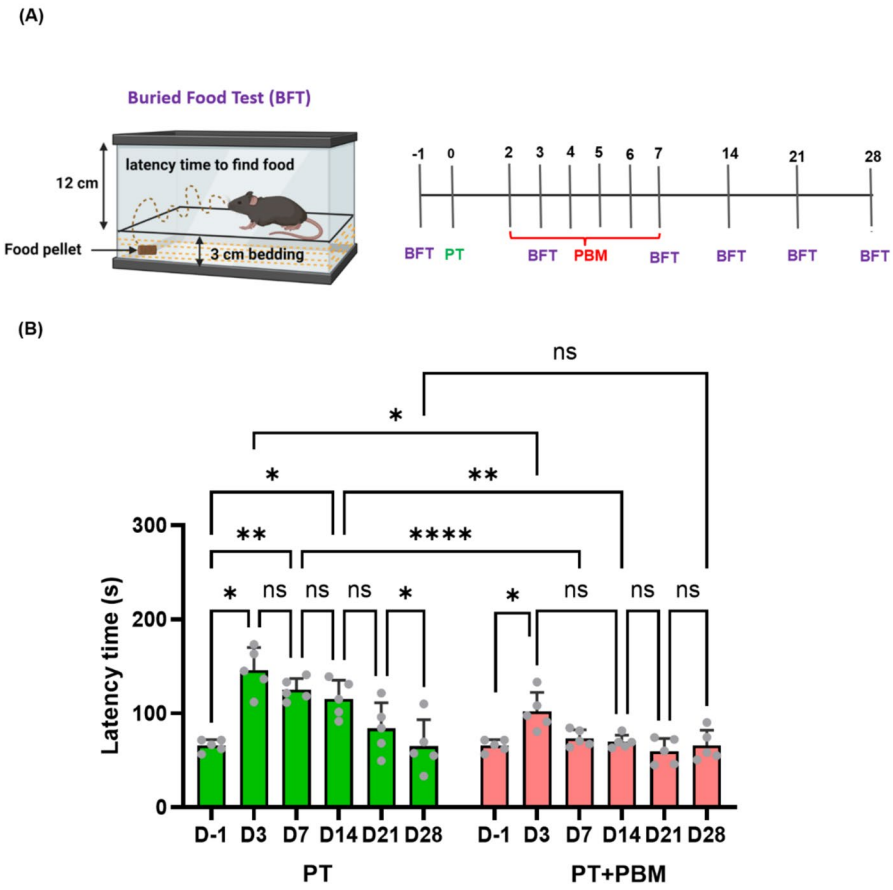

Fig. 2 Impact of PBM on the olfactory function following PT from early to late stages. **A** Schematic representation of the buried food test (BFT) protocol used to assess olfactory function in mice after PT stroke (top panel). The latency to find the food pellet was recorded from day -1 (baseline) until day 28 post-PT. PBM treatment was administered daily from day 2 to day 7 post-PT (red line). **B** Olfactory function in the PT and PT + PBM groups from baseline until day 28 (*$P < 0.05$, **$P < 0.01$, ****$P < 0.0001$, ns = not significant). $n = 5$ per group

Gene Expression Profiling in the OB Post-PT and PBM Therapy

To explore the molecular mechanisms underlying the effects of PBM on stroke recovery, RNA sequencing (RNA-seq) was conducted to profile gene expression in the olfactory bulb (OB) after PT. Figure 4A–C presents heatmaps of the top 40 differentially expressed genes (DEGs). Hierarchical clustering in these heatmaps further demonstrates that both PT and PT + PBM groups show significant transcriptional differences compared to control, with PBM-treated animals showing a unique transcriptional profile. Notably, several genes involved in neuroprotection, inflammation, and recovery are differentially expressed, implying that PBM modulates key recovery pathways in the brain.

Figure 4D presents Venn diagrams of deregulated genes and top-regulated genes between the different experimental groups. In the upregulated gene comparison (left), the PT + PBM vs. control group shares 2084 DEGs with the PT vs. control group, suggesting that many of the genes activated in stroke are similarly modulated by PBM. However, 671 genes are upregulated in the PT + PBM group, indicating that PBM triggers distinct molecular responses. Among these top-regulated genes, GPR39 stands out as one of the top-upregulated genes following PBM treatment, highlighting its potential role in enhancing neuroprotection and recovery after ischemic injury.

The downregulated gene comparison (right) shows that 234 genes are distinctly downregulated in the PT + PBM group compared to the control, further supporting the idea that PBM specifically modulates certain pathways involved in stroke recovery.

To further explore the role of key genes in the PBM-mediated recovery process, we conducted quantitative RT-qPCR analysis on *GPR39* and *OR4M1*, two genes with known neuroprotective functions. As shown in Fig. 4E, *GPR39* expression was significantly higher in the PBM-treated group at day 7 post-PT compared to the PT-only group. This finding suggests that *GPR39* may play a critical role in mediating the beneficial effects of PBM in the acute phase of stroke recovery. By day 28, *GPR39* expression levels in the PBM group had decreased and were closer to baseline levels, indicating that the gene's upregulation is transient and occurs primarily during the early stages of recovery.

Similarly, *OR4M1*, which is associated with neuroprotection in traumatic brain injury, exhibited a similar expression pattern. *OR4M1* expression was comparable between the PT and PT + PBM groups at day 7, suggesting that it is part of

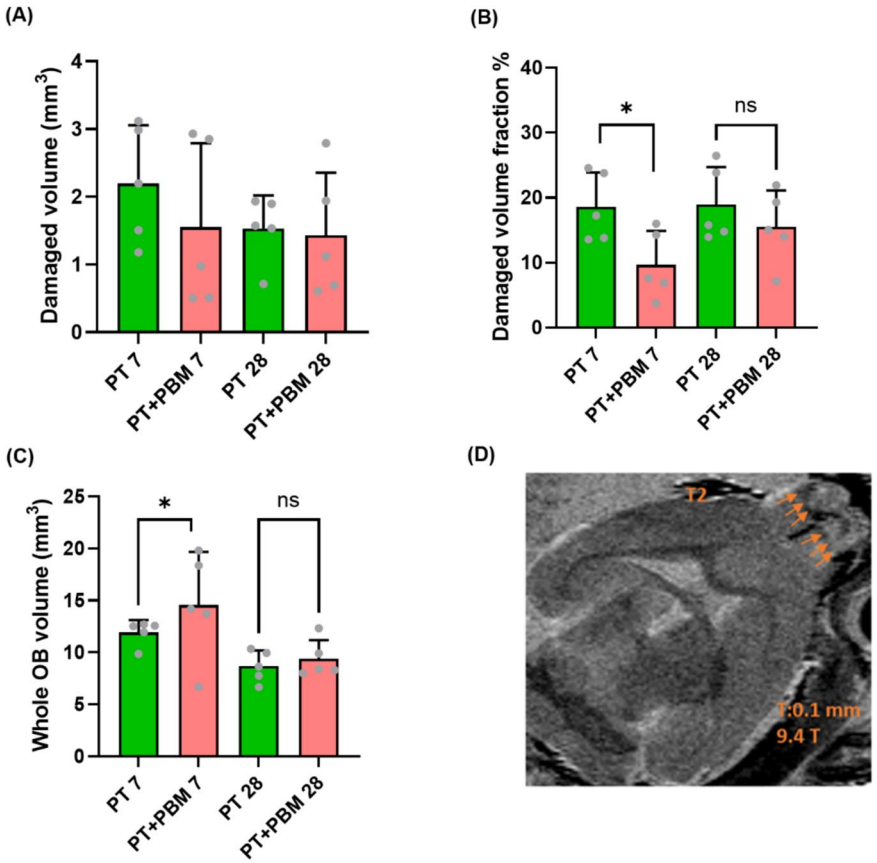

Fig. 3 MRI imaging of the olfactory bulb post-PT and post-PBM treatment. **A** Damaged volume (mm^3) of the olfactory bulb at 7 and 28 days post-PT for both PT and PT + PBM groups. **B** Damaged volume fraction of the olfactory bulb at day 7 and day 28. **C** Whole OB volume (mm^3) for PT and PT + PBM groups at day 7 and day 28 post-PT. **D** Representative MRI image (T2) of the olfactory bulb, with arrows indicating the damaged region. Thickness, 0.1 mm. (*$P < 0.05$, ns = not significant). $n = 5$ per group

the natural recovery process post-stroke. By day 28, *OR4M1* expression levels returned to baseline in both groups, indicating that PBM does not have a sustained effect on this gene in the later stages of recovery.

In summary, these results indicate that PBM induces significant transcriptional changes in the olfactory bulb post-stroke, with upregulation of genes like *GPR39* and *OR4M1* during the early recovery phase. The transient nature of these changes suggests that PBM's therapeutic effects may be time-sensitive, targeting specific pathways involved in the acute response to ischemic injury.

Discussion

This study aimed to evaluate the therapeutic potential of photobiomodulation (PBM) in treating olfactory dysfunction following ischemic stroke induced by photothrombosis (PT) in the olfactory bulb (OB). Our results demonstrated that PBM significantly accelerated the recovery of olfactory function in the early stages post-PT, with full recovery by day 14 sustained through day 28. Despite the restoration of olfactory function, MRI imaging revealed persistent infarction on day 28, suggesting that PBM may facilitate functional improvements through mechanisms other than direct tissue repair.

Although PBM has gained increasing attention for treating various pathological disorders, including neurodegenerative diseases, some studies have shown less significant effects. For example, Sipion et al. reported no significant differences between the PBM-treated Alzheimer's disease (AD) group and the untreated AD group in behavioral tests. Additionally, histological analyses revealed no notable differences in amyloid load, neuronal loss, or microglial response between the two groups [17]. It was reported also that PBM has no effects on the prefrontal cortex and hippocampus development in young rats [18]. Taken together, further studies are needed to provide more definitive evidence on whether PBM has positive or neutral effects.

The restoration of olfactory function observed in our study aligns with the notion that PBM can promote functional recovery through neuroplasticity and modulation of the neural microenvironment. Interestingly, some studies have reported structural repair or neurogenesis following PBM [19]. Our MRI results did not show significant tissue regeneration in the OB. This discrepancy may be due to differences in experimental models, PBM parameters, or the specific brain regions examined. It suggests that PBM may enhance functional recovery by facilitating synaptic

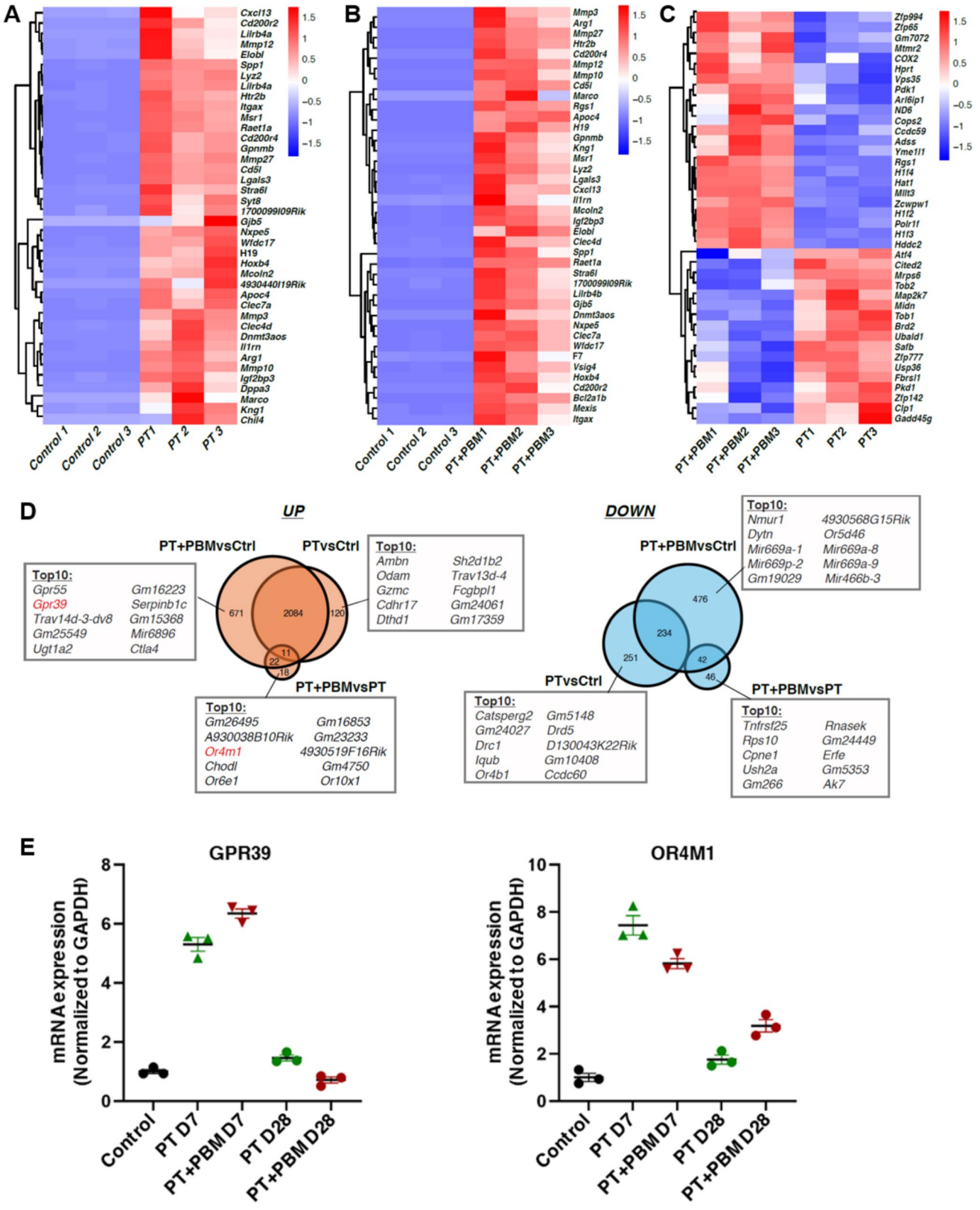

Fig. 4 Transcriptomic analysis of PBM in PT ischemic stroke model. **A**–**C** Heatmaps showing the top 40 DEGs across groups, clustered by gene expression profiles. **A** PT + PBM vs. control, **B** PT vs. control, and **C** PT + PBM vs. PT. **D** Venn diagrams of overlapping and top upregulated and downregulated genes with the top 10 DEGs for each comparison. **E** Quantitative RT-qPCR of GPR39 and OR4M1 mRNA expression levels normalized to GAPDH, in control, PT, and PT + PBM groups at day 7 and day 28 post-PT. $n = 3$ per group

plasticity and compensatory neural network reorganization [20], rather than directly repairing damaged tissue [21]. PBM may enhance synaptic plasticity, strengthen existing neural circuits, or promote functional reorganization to compensate for damaged areas. Such mechanisms have been proposed in studies of neural plasticity and rehabilitation after stroke [22]. For example, Murphy and Corbett [23] discussed how post-stroke rehabilitation can harness neural plasticity to improve functional outcomes, and our findings suggest that PBM may act as a catalyst in this process.

Our immunohistochemical analyses revealed that PBM effectively reduced astrocyte activation, as indicated by decreased GFAP expression, at both early and late stages post-PT. Reactive astrocytes can contribute to glial scar formation and inhibit neuronal regeneration [24]. By attenuating astrocyte activation, PBM may create a more permissive environment for neuronal recovery and synaptic plasticity. This finding is consistent with other studies reporting that PBM can modulate glial cell activity and reduce neuroinflammation [25].

Interestingly, PBM had a limited effect on microglia activation, as evidenced by minimal changes in IBA-1 expression. Microglia play complex roles in the central nervous system, contributing to both injury and repair processes [26]. Delayed microglial activation has been detected in regions distant from the infarct and is thought to contribute to gradual and progressive neurodegeneration over time [27]. The lack of significant impact on microglia suggests that PBM's primary mechanism may involve astrocytic pathways rather than microglial modulation. Alternatively, the timing of our assessments may not have captured transient changes in microglial activity, and future studies could explore this aspect further.

Our RNA-seq and RT-qPCR analyses identified significant upregulation of the neuroprotective gene *Gpr39* in PBM-treated mice at day 7 post-PT. *Gpr39* has been implicated in regulating microvascular perfusion, neuronal survival, and neurogenesis after ischemic injury [28]. The transient upregulation of *Gpr39* suggests that PBM enhances endogenous recovery mechanisms during the critical early period following stroke. Additionally, the upregulation of *Or4m1*, an olfactory receptor gene associated with neural repair, indicates that PBM may influence sensory-specific pathways to promote functional recovery [29]. These molecular changes may underlie the observed functional improvements without apparent structural repair.

Our study presents novel insights into the therapeutic effects of PBM on olfactory dysfunction post-stroke. By focusing on the OB, a region critical for olfaction and susceptible to ischemic injury, we highlight the potential of PBM to address sensory deficits that are often overlooked in stroke recovery. The identification of specific genes modulated by PBM provides a foundation for understanding the molecular basis of its therapeutic actions and may guide the development of targeted interventions.

However, several limitations of this study should be acknowledged. The use of bulk RNA-seq limits our ability to attribute gene expression changes to specific cell types within the OB. Single-cell RNA-seq or spatial transcriptomics would provide more detailed insights into the cellular mechanisms underlying PBM's effects [4, 30]. Additionally, we did not assess functional connectivity or synaptic changes that may contribute to the recovery of olfactory function. Electrophysiological recordings or advanced imaging techniques such as functional MRI could address this gap.

Furthermore, while our study focused on the acute and subacute phases post-stroke, longer-term assessments are needed to determine the durability of PBM's effects and its impact on chronic recovery stages. Investigating different PBM parameters, such as wavelength, dosage, and treatment duration, may optimize therapeutic outcomes. Finally, translating these findings to clinical practice requires caution. Differences between animal models and human pathology necessitate rigorous clinical trials to evaluate PBM's safety and efficacy in stroke patients with olfactory dysfunction.

Conclusion

Our study demonstrates that PBM therapy accelerates the recovery of olfactory function in the early stages following ischemic stroke in a mouse olfactory bulb. We observed that PBM reduces astrocyte activation and enhances the expression of neuroprotective genes, such as *Gpr39* during the acute recovery phase. These findings suggest that PBM may facilitate functional recovery by modulating the neuroinflammatory environment and promoting endogenous protective mechanisms. By offering novel insights into the molecular and cellular effects of PBM, our study provides a foundation for future research aimed at developing effective therapies for sensory deficits following stroke.

Supplementary Information The online version contains supplementary material available at https://doi.org/10.1007/s12975-025-01343-3.

Author Contribution R.A.S. performed experimental work, analyzed data, and wrote the main manuscript text. A.E. analyzed RNA sequencing results and performed RT-qPCR experiments. F.D.N.D., K.A., and S.M.A.S. assisted with experimental work. K.A. also performed CD31 analysis. J.Y. and J.P. analyzed RNA sequencing data. K.H.L. and S.M.A.S. performed histopathological staining. Y.R.K. conducted MRI scanning. H.S.K., S.S.K, Y.R.K., and E.C. conceived and supervised the project. All authors reviewed the manuscript.

Funding The research was supported by the National Research Foundation of Korea (NRF) grant funded by the Korean government (MSIT) (no. RS-2023–00264409, no. RS-2023–00302281) and the Brain Pool

program funded by the Ministry of Science and ICT through the NRF of Korea (RS-2023–00304323).

Data Availability All the raw data could be uploaded in the supplementary materials upon request.

Declarations

Ethical Approval All experimental protocols followed the guidelines of the Institutional Animal Care and Use Committee (IACUC) at Gwangju Institute of Science and Technology (GIST), Korea. The experimental protocols were approved by the GIST IACUC under protocol # GIST-2024–046.

Conflict of Interest The authors declare no competing interests.

References

1. Cleland TA, Linster C. Computation in the olfactory system. Chem Senses. 2005;30(9):801–13.
2. Shalaby RA, et al. Photobiomodulation therapy restores olfactory function impaired by photothrombosis in mouse olfactory bulb. Experimental Neurology. 2023;367:114462.
3. Brann JH, Firestein SJ. A lifetime of neurogenesis in the olfactory system. Front Neurosci. 2014;8:182.
4. Zheng K, et al. Single-cell RNA-seq reveals the transcriptional landscape in ischemic stroke. J Cereb Blood Flow Metab. 2022;42(1):56–73.
5. Yang L, et al. Photobiomodulation therapy promotes neurogenesis by improving post-stroke local microenvironment and stimulating neuroprogenitor cells. Exp Neurol. 2018;299(Pt A):86–96.
6. Feng Y, et al. Photobiomodulation inhibits ischemia-Induced brain endothelial senescence via endothelial nitric oxide synthase. antioxidants (Basel). 2024;13(6). https://doi.org/10.3390/antiox13060633
7. Purushothuman S, et al. Photobiomodulation with near infrared light mitigates Alzheimer's disease-related pathology in cerebral cortex - evidence from two transgenic mouse models. Alzheimers Res Ther. 2014;6(1):633.
8. Wang M, et al. Non-invasive modulation of meningeal lymphatics ameliorates ageing and Alzheimer's disease-associated pathology and cognition in mice. Nat Commun. 2024;15(1):1453.
9. Naeser MA, et al. Improved cognitive function after transcranial, light-emitting diode treatments in chronic, traumatic brain injury: two case reports. Photomed Laser Surg. 2011;29(5):351–8.
10. Chao LL, et al. Changes in brain function and structure after self-administered home photobiomodulation treatment in a concussion case. Front Neurol. 2020;11:952.
11. Carmichael ST. Rodent models of focal stroke: size, mechanism, and purpose. NeuroRx. 2005;2(3):396–409.
12. Weber RZ, et al. Characterization of the blood brain barrier disruption in the photothrombotic stroke model. Front Physiol. 2020;11:586226.
13. Rust R. Ischemic stroke-related gene expression profiles across species: a meta-analysis. J Inflamm (Lond). 2023;20(1):21.
14. Xu Y, et al. GPR39 knockout worsens microcirculatory response to experimental stroke in a sex-dependent manner. Transl Stroke Res. 2023;14(5):766–75.
15. Zhao W, et al. Decreased level of olfactory receptors in blood cells following traumatic brain injury and potential association with tauopathy. J Alzheimers Dis. 2013;34(2):417–29.
16. Yang M, Crawley JN. Simple behavioral assessment of mouse olfaction. Curr Protoc Neurosci. 2009;Chapter 8: p. Unit 8 24. https://doi.org/10.1002/0471142301.ns0824s48
17. Sipion, M., et al., A randomized, blinded study of photobiomodulation in a mouse model of Alzheimer's disease showed no preventive effect. Sci Rep. 2023:13(1). https://doi.org/10.1038/s41598-023-47039-2
18. Gutierrez-Menendez A, et al. No effects of photobiomodulation on prefrontal cortex and hippocampal cytochrome C oxidase activity and expression of c-Fos protein of young male and female rats. Front Neurosci. 2022;16. https://doi.org/10.3389/fnins.2022.897225
19. Salehpour F, Hamblin MR, DiDuro JO. Rapid reversal of cognitive decline, olfactory dysfunction, and quality of life using multi-modality photobiomodulation therapy: case report. Photobiomodul Photomed Laser Surg. 2019;37(3):159–67.
20. Grefkes C, Fink GR. Recovery from stroke: current concepts and future perspectives. Neurol Res Pract. 2020;2:17.
21. Raffin E, Hummel FC. Restoring motor functions after stroke: multiple approaches and opportunities. Neuroscientist. 2018;24(4):400–16.
22. Hofer AS, Schwab ME. Enhancing rehabilitation and functional recovery after brain and spinal cord trauma with electrical neuromodulation. Curr Opin Neurol. 2019;32(6):828–35.
23. Murphy TH, Corbett D. Plasticity during stroke recovery: from synapse to behaviour. Nat Rev Neurosci. 2009;10(12):861–72.
24. Guttenplan KA, et al. Neurotoxic reactive astrocytes induce cell death via saturated lipids. Nature. 2021;599(7883):102–7.
25. Wang X, et al. Photobiomodulation inhibits the activation of neurotoxic microglia and astrocytes by inhibiting Lcn2/JAK2-STAT3 crosstalk after spinal cord injury in male rats. J Neuroinflammation. 2021;18(1):256.
26. Qin C, et al. Dual functions of microglia in ischemic stroke. Neurosci Bull. 2019;35(5):921–33.
27. Walberer M, et al. In-vivo detection of inflammation and neurodegeneration in the chronic phase after permanent embolic stroke in rats. Brain Res. 2014;1581:80–8.
28. Cao B, Wang J, Feng J. Signaling pathway mechanisms of neurological diseases induced by G protein-coupled receptor 39. CNS Neurosci Ther. 2023;29(6):1470–83.
29. Liu X, et al. Traumatic brain injury-induced inflammatory changes in the olfactory bulb disrupt neuronal networks leading to olfactory dysfunction. Brain Behav Immun. 2023;114:22–45.
30. Zheng GX, et al. Massively parallel digital transcriptional profiling of single cells. Nat Commun. 2017;8:14049.